# Development of quantum nonintegrability displayed in effective Hamiltonians: A three-level Lipkin model

Xu Gong-ou
*Department of Physics, Nanjing University, Nanjing 210008, China;*
*Department of Modern Physics, Lanzhou University, Lanzhou 730000, China;*
*National Laboratory of Heavy Ion Accelerator, Lanzhou 730000, China;*
*and Institute of Nuclear Research, Shanghai, Academia Sinica, Shanghai 201800, China*

Gong Jiang-bin
*Department of Physics, Nanjing University, Nanjing 210008, China*

Wang Wen-ge
*Institute of Nuclear Research, Shanghai, Academia Sinica, Shanghai 201800, China*

Yang Ya-tian
*Department of Physics, Fujian Normal University, Fuzhou 350007, China*

Fu De-ji
*China Center of Advanced Science and Technology (World Laboratory), Beijing, China*
*and Institute of Nuclear Research, Shanghai, Academia Sinica, Shanghai 201800, China*
(Received 4 February 1994; revised manuscript received 20 June 1994)

The transition to chaos as the development of global nonintegrability in a three-level Lipkin model is investigated numerically. With effective Hamiltonians for different energy regions it is possible to study local statistical behaviors of the system in the corresponding energy regions. Behaviors of its classical counterparts are also given for comparison. The dynamical origin of statistical properties of effective Hamiltonian matrices is qualitatively explained. The question of what are the members of the Gaussian orthogonal ensemble is also discussed.

PACS number(s): 05.45.+b, 03.65.−w

## I. INTRODUCTION

It is well known, for autonomous quantum systems with their classical counterparts fully chaotic that the statistical properties of the energy spectra are predicted by the Gaussian orthogonal ensemble (GOE) [1]. There are also good arguments to associate regular spectra with classical integrable systems [2]. If the Hamiltonian $H^0$ is completely integrable and $H$ gives GOE statistics, then the statistics for the eigenenergies of the Hamiltonian

$$H(\lambda)=H^0+\lambda(H-H^0) \tag{1}$$

become different from the Wigner distribution and closer to the Poisson distribution as $\lambda$ decreases from 1 to 0. The dynamics of the intermediate regime is still poorly understood [3] because the universal theory of random matrices gives us no clue concerning the connection of the two types of statistics. The deviation from GOE statistics merely indicates that the relevant Hamiltonian matrices fail to meet the requirements of GOE.

Berry and Robnik [4], based on semiclassical considerations, suggested that the intermediate statistics are due to the coexistence of integrable and nonintegrable regions and can be explained as a superposition of the two kinds of well-known statistics; while Brody [5] introduced phenomenologically the spacing distribution just interpolating between the Poisson and Wigner distribution by introducing an interpolation parameter.

Recently, such deviations from GOE statistics were explained in more detail as due to partial integrability of systems $H(\lambda)$ and characterized with the mean $\nu$ of the $\chi^2_\nu$ distribution of eigenvectors together with the mean Lyapunov exponent of the classical limit [6], or with the mean distributedness of eigenvectors [7]. Since conventional statistical analyses for schematic models always cover all the eigenstates, corresponding mean values have to be introduced to take into account the different local dynamical properties of Hamiltonian systems. Different from schematic models, local dynamical properties were always emphasized for cases of experimental nuclear data. Haq, Pandey, and Bohigs [8] analyzed the whole body of high-quality data, 1407 resonances corresponding to 30 sequences of 27 different nuclei. Astonishingly good agreement was found between the experimental data and the GOE statistics. On the other hand, Garrett *et al.* [9] analyzed spectra of rare-earth nuclei in the vicinity of the yrast line and found near-Poissonian statistics indicating the regular motion of collective rotational bands.

Several authors have already noticed these points. Brown and Bertsch [10] tried to determine to what extent

 

a realistic nuclear Hamiltonian can be viewed as just a representative of a random matrix ensemble by investigating the distribution of basis-vector amplitudes in realistic $s$-$d$ shell-model eigenfunctions, but they concluded that the shell-model Hamiltonian does not look at all like a representative of the random matrix ensemble. It has been suggested [11,12] that a useful parameter for determining the applicability of random matrix results is the ratio of the rms value of the off-diagonal matrix element to the average level spacing; while Meredith, Koonin, and Zirnbauer [13] studied in detail the connection between chaotic classical motion and quantum spectral and overlap statistics. However, the question of what is a member of the random matrix ensemble is still unanswered.

Considering the above-mentioned points together, we take the effective Hamiltonians for different energy regions of systems with respective local mean properties removed by an unfolding process as members of GOE and examine whether they fulfill the following two statistical requirements: (a) all the independent elements of the Hermitian matrix are independent random variables; (b) the randomness property is invariant to arbitrary orthogonal transformations. The effective Hamiltonians related to different energy regions are explicitly obtained with a decoupling transformation, and then their randomness properties are studied with eigenvector statistics. Based on numerical results, we are able to confirm that the unfolded effective Hamiltonian matrices are really members of GOE and conclude further that the quantum manifestation of the classical transition from regularity to chaos is characterized by the broadening of the energy region over which the effective Hamiltonians are all random.

There remains the problem of what is the dynamical origin of the randomness of effective Hamiltonian matrices. This is answered with the dynamical property of global nonintegrability. Hence the transition from order to chaos can be regarded as a manifestation of the development of global nonintegrability.

This article is organized as follows. In Sec. II, the nearest neighbor spacing statistics for the energy spectra of a three-level Lipkin model [14] are presented. In Sec. III, the effective Hamiltonian matrices for different energy intervals of the system $H(\lambda)$ and their statistical behaviors are studied. In Sec. IV, parallel results of the classical counterparts for demonstrating the quantum classical correspondence are given. In Sec. V, the statistical requirements of GOE are discussed from the dynamical properties of global nonintegrability of the systems. Conclusions are given in the last section.

## II. SPECTRAL STATISTICS OF $H(\lambda)$

The Hamiltonian of the three-level Lipkin model is of the following form:

$$H(\lambda)=H^0+\lambda(H-H^0)\ , \tag{2}$$

$$H^0=\epsilon_1 K_{11}+\epsilon_2 K_{22}-\kappa_2(K_{20}K_{20}+\text{H.c.})\ , \tag{3}$$

$$H-H^0=-\kappa_1(K_{10}K_{10}+\text{H.c.})+\mu_1(K_{21}K_{20}+\text{H.c.})+\mu_2(K_{12}K_{10}+\text{H.c.})\ , \tag{4}$$

where

$$K_{ij}=\sum_{\alpha=1}^{\Omega} a_{i\alpha}^{\dagger}a_{j\alpha},\quad i,j=0,1,2 \tag{5}$$

$$\epsilon_1=1.0,\quad \epsilon_2=1.6\quad \kappa_1=0.13,\quad \kappa_2=0.21\ ,$$
$$\mu_1=0.23,\quad \mu_2=0.183,\quad \Omega=30\ . \tag{6}$$

The number of particles is taken as 30. Only collective

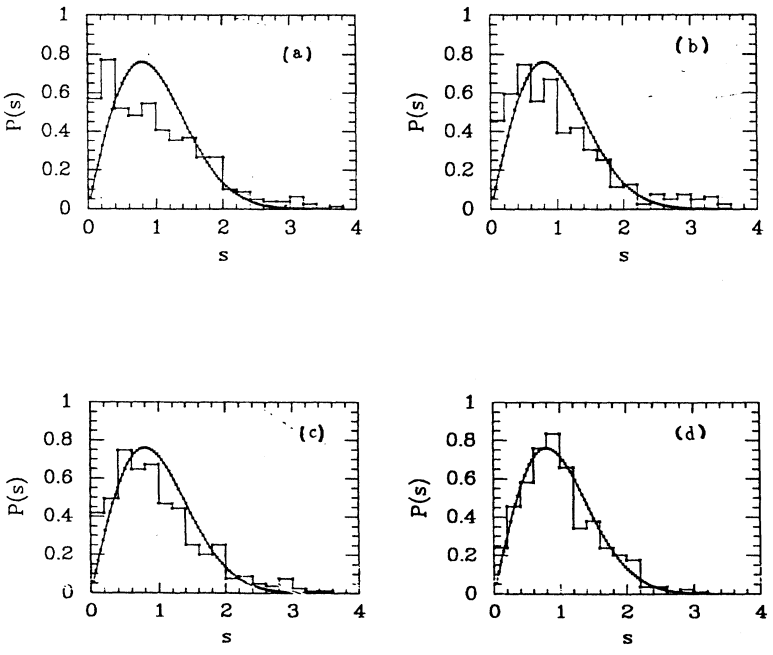


FIG. 1. The nearest neighbor statistics $P(s,\lambda)$ of the system $H(\lambda)$ for (a) $\lambda=0.08$; (b) $\lambda=0.24$; (c) $\lambda=0.48$; (d) $\lambda=0.78$.

motions based on the ground state are considered. Therefore the dynamical group is the SU(3) group. The Hamiltonian is time-reversal invariant.

In Fig. 1, the transition of the spectral statistics is illustrated. When the perturbation strength represented by $\lambda$ is small, the nearest neighbor spacing statistics show regular properties. Then with the increasing of $\lambda$, the spectral statistics fit the theoretical distributions predicted by GOE better and better. Obviously when $\lambda$ is larger than 0.78, the generic behaviors of the model Hamiltonian can be well described by the random-matrix theory. In fact, as we will see, this case corresponds to a fully chaotic classical limit.

## III. EFFECTIVE HAMILTONIAN MATRICES AND THEIR STATISTICAL PROPERTIES

Suppose $|\phi_i^0\rangle$ are eigenstates of $H^0$, and $|\phi_i(\lambda)\rangle$ are eigenstates of $H(\lambda)$ with eigenvalues $E_i(\lambda)$. $|\phi_i(\lambda)\rangle$ vary continuously with $\lambda$ and satisfy the following condition:

$$\lim_{(\lambda\to 0)} |\phi_i(\lambda)\rangle = |\phi_i^0\rangle \ . \tag{7}$$

Thus the above two sets of eigenstates have a one to one correspondence. From them we can define an orthogonal transformation $U(\lambda,0)$ as follows:

$$U(\lambda,0)=\sum_i |\phi_i(\lambda)\rangle\langle\phi_i^0| \ . \tag{8}$$

With such an orthogonal transformation, the Hamiltonian matrix is diagonalized.

$$\sum_{k,l}\langle\phi_j^0|U^\dagger(\lambda,0)|\phi_l^0\rangle\langle\phi_l^0|H(\lambda))|\phi_k^0\rangle\langle\phi_k^0|U(\lambda,0)|\phi_i^0\rangle = E_i(\lambda)\delta_{ji} \ . \tag{9}$$

In order to show the local behavior of the energy spectrum, we divide the whole $N$-dimensional Hilbert space into $K$ energy regions with $\Delta N$ eigenstates of $H(\lambda)$ in each energy region, and try to obtain the effective Hamiltonian matrix in block form with each block for each energy region. This can be achieved by the decoupling transformation [15], or speaking alternatively, by the coset resolution of the orthogonal transformation matrix $U(\lambda,0)=U_l(\lambda)U_c(\lambda,0)$ where $U(\lambda,0)$ and $U_l(\lambda)$ are elements of the SO($N$) group and SO($\Delta N$) $\otimes$SO($\Delta N$)$\otimes\cdots\otimes$SO($\Delta N$) subgroup respectively, while $U_c(\lambda,0)$ is an element of the quotient SO($N$)/[SO($\Delta N$)$\otimes\cdots\otimes$SO($\Delta N$)]. The number of independent matrix elements of $U(\lambda,0)$, $U_l(\lambda)$, and $U_c(\lambda,0)$ are $\frac{1}{2}N(N+1)$, $(K/2)\Delta N(\Delta N+1)$, and $\frac{1}{2}N(N+1)-(K/2)\Delta N(\Delta N+1)$, respectively. If the orthogonal transformation matrix $U(\lambda,0)$ is given, matrices $U_l(\lambda)$ and $U_c(\lambda,0)$ are uniquely determined. We define

$$|\eta_k(\lambda)\rangle = U_c(\lambda,0)|\phi_k^0\rangle \ . \tag{10}$$

With the resolution and the completeness relation $\sum_k|\eta_k\rangle\langle\eta_k|=1$, Eq. (9) can be rewritten as

$$\sum_{k,l}\langle\eta_j(\lambda)|U_l^\dagger(\lambda)|\eta_l(\lambda)\rangle\langle\eta_l(\lambda)|H(\lambda)|\eta_k(\lambda)\rangle\langle\eta_k(\lambda)|U_l(\lambda)|\eta_i(\lambda)\rangle = E_i\delta_{jk} \ . \tag{11}$$

Since $\langle\eta_l(\lambda)|H(\lambda)|\eta_k(\lambda)\rangle$ is diagonalized with the transformation matrix $\langle\eta_k(\lambda)|U_l(\lambda)|\eta_l(\lambda\rangle$ which is in block form, $\langle\eta_l(\lambda)|H(\lambda)|\eta_k(\lambda)\rangle$ must be a block matrix. Hence in the representation $\eta_l(\lambda)$.

$$H(\lambda)=H_{\text{eff};1}(\lambda)\oplus H_{\text{eff};2}(\lambda)\oplus\cdots \ , \tag{12}$$

where

$$H_{\text{eff},\mu}(\lambda)=\langle\eta_l(\lambda)|H(\lambda)|\eta_k(\lambda)\rangle, \quad l,k\in[\mu] \tag{13}$$

are just the required effective Hamiltonians for different energy regions.

From Eqs. (10)–(13) we see clearly that $|\eta_i(\lambda)\rangle$ form the bases of the decoupled representation and $U_c(\lambda,0)$ is the corresponding decoupling transformation. Based on this fact, we would try to determine $|\eta_k(\lambda)\rangle$ ($k$ in energy region $\mu$) with the projection operator

$$P_\mu(\lambda)=\sum_{i\in[\mu]}|\phi_i(\lambda)\rangle\langle\phi_i(\lambda)| \ . \tag{14}$$

A set of orthogonal states is generally not orthogonal after the projection. It is only possible for a special set of orthogonal states to keep their orthogonality after the projection. Let

$$|\phi_a^0\rangle=\sum_{i\in[\mu]}C_i^a|\phi_i^0\rangle, \quad a=1,\ldots,\Delta N\in[\mu] \tag{15}$$

be such a set of orthogonal states in the corresponding subspace defined by

$$P_\mu(0)=\sum_{i\in[\mu]}|\phi_i^0\rangle\langle\phi_i^0|=\sum_{a\in[\mu]}|\phi_a^0\rangle\langle\phi_a^0| \ . \tag{16}$$

Obviously, we have the following orthogonality and completeness relations:

$$\sum_{i\in[\mu]}C_i^aC_i^b=\delta_{ab} \ , \tag{17}$$

$$\sum_{a\in[\mu]}C_i^aC_j^a=\delta_{ij} \ . \tag{18}$$

Requiring that $P_\mu(\lambda)|\phi_a^0\rangle$ and $P_\mu(\lambda)|\phi_b^0\rangle$ remain orthogonal,

$$\langle\phi_b^0|P_\mu(\lambda)P_\mu(\lambda)|\phi_a^0\rangle=\langle\phi_b^0|P_\mu(\lambda)|\phi_a^0\rangle=l_a(\lambda)\delta_{ba} \ , \tag{19}$$

we have

$$\sum_{j,k\in[\mu]}C_j^b\langle\phi_j^0|P_\mu(\lambda)|\phi_i^0\rangle C_i^a=l_a(\lambda)\delta_{ba} \ . \tag{20}$$

Multiplying both sides by $C_k^b$ and summing over $b$, we have

$$\sum_{i\in[\mu]} \langle \phi_k^0|P_\mu(\lambda)|\phi_i^0\rangle C_i^a = l_a(\lambda) C_k^a \ . \tag{21}$$

Solving the set of equations, we obtain the corresponding two sets of orthonormal states $|\phi_a^0\rangle$ and $|\phi_a(\lambda)\rangle$, where

$$|\phi_a(\lambda)\rangle = [l_a(\lambda)]^{-1/2} P_\mu(\lambda)|\phi_a^0\rangle \ . \tag{22}$$

$P_\mu(\lambda)$ in (14) can then also be written as

$$P_\mu(\lambda) = \sum_{a\in[\mu]} |\phi_a(\lambda)\rangle\langle\phi_a(\lambda)| \ . \tag{23}$$

The same process can be carried out for all energy regions to obtain the corresponding set of orthonormal states $|\phi_a^0\rangle$ and $|\phi_a(\lambda)\rangle$ for all energy regions. Thus the decoupling transformation $U_c(\lambda,0)$ in (10) can be expressed as

$$U_c(\lambda,0) = \sum_a |\phi_a(\lambda)\rangle\langle\phi_a^0| \ . \tag{24}$$

In determining $U_c(\lambda,0)$, only the projection operators $P_\mu(\lambda)$ for different energy regions have been used. Though all the states $|\phi_i(\lambda)\rangle$ have been involved, they appear in the projection operator $P_\mu(\lambda)$ not individually. $P_\mu(\lambda)$ can be written in different forms, e.g., as (14) and (23). Hence $U_c(\lambda,0)$ thus determined involves only $\frac{1}{2}N(N+1)-(K/2)\Delta N(\Delta N+1)$ independent elements. In short, $U_c(\lambda,0)$ is determined merely from the geometrical relation between the corresponding subspaces defined by $P_\mu(\lambda)$ and $P_\mu(0)$, leaving the further diagonalization of the effective Hamiltonian perfectly to the orthogonal transformation $U_l(\lambda)$. In this way, the decoupled representation is closest to the original integrable $H^0$ representation and farthest from the eigenrepresentation of $H(\lambda)$.

Having obtained the effective Hamiltonian in the decoupled representation for different energy regions, the eigensolutions can be readily found. The eigenenergies $E_i(\lambda)$ are representation independent, though the eigenstates of $H_{\text{eff};\mu}(\lambda)$ are expressed as

$$|\phi_{i\in[\mu]}(\lambda)\rangle = \sum_{j\in[\mu]} |\eta_j(\lambda)\rangle\langle\eta_j(\lambda)|\phi_i(\lambda)\rangle \ . \tag{25}$$

In fact, $\langle\eta_j(\lambda)|\phi_i(\lambda)\rangle$ can be calculated from results of $|\phi_i(\lambda)\rangle$ and $|\eta_j(\lambda)\rangle$ in the original $H^0$ representation; the further diagonalization of the localized effective Hamiltonian matrices is unnecessary.

There remains the problem of whether $H_{\text{eff};\mu}(\lambda)$ can be treated as members of the (GOE). In principle, both the eigenenergies and eigenstates can be used for answering the above question. But the eigenstates have many more independent elements than the eigenenergies, and can therefore be analyzed statistically for each energy region individually. Moreover, for answering the above question, it is only necessary to compare the statistical distribution of the magnitude of $\langle\eta_l(\lambda)|\phi_i(\lambda)\rangle$ or $|\langle\eta_l(\lambda)|\phi_i(\lambda)\rangle|^2$ with that of completely random variables. Such a comparison should be performed with a representation sufficiently far away from the eigenrepresentation of $H(\lambda)$. The decoupled representation closest to the original integrable $H^0$ representation and farthest from the eigenrepresentation of $H(\lambda)$ is of course the best choice. However, other decoupled representations sufficiently different from the eigenrepresentation of $H(\lambda,0)$ also serve the purpose. We have also considered a decoupled representation determined by the projection operators $P_\mu(\lambda)$ together with the Schmidt method of orthogonalization for eigenvector analyzes; the results are almost unaltered.

Results of $\chi_\nu^2$ analyses of eigenvectors localized in different energy regions are shown in Figs. 2–5 corresponding to four values of $\lambda$, respectively. Three typical energy regions with the mean energy around 20.0, 55.0, and 75.0 are chosen for each ease. The effective Hamiltonians are all 31 dimensional. For the case $\lambda=0.08$ in

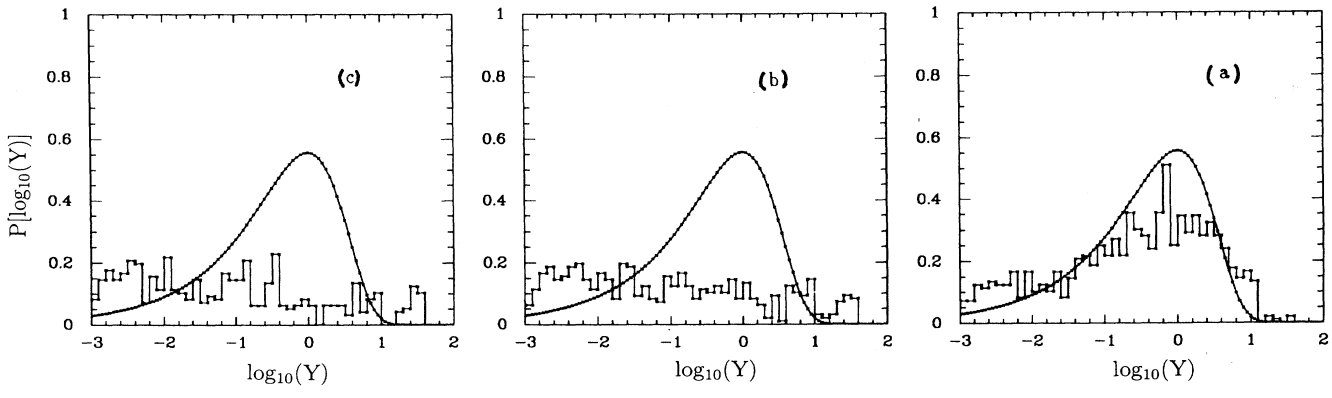


FIG. 2. Histograms of distributions for the components of eigenvectors of effective Hamiltonians related to different energy regions for the case $\lambda=0.08$. The effective Hamiltonian for a certain energy region is 31 dimensional. The solid lines denote the $\chi^2_{\nu=1}$ distribution. Graphs denoted by (a), (b), and (c) are for effective Hamiltonians with the mean energy around 20.0, 55.0, and 75.0, respectively.

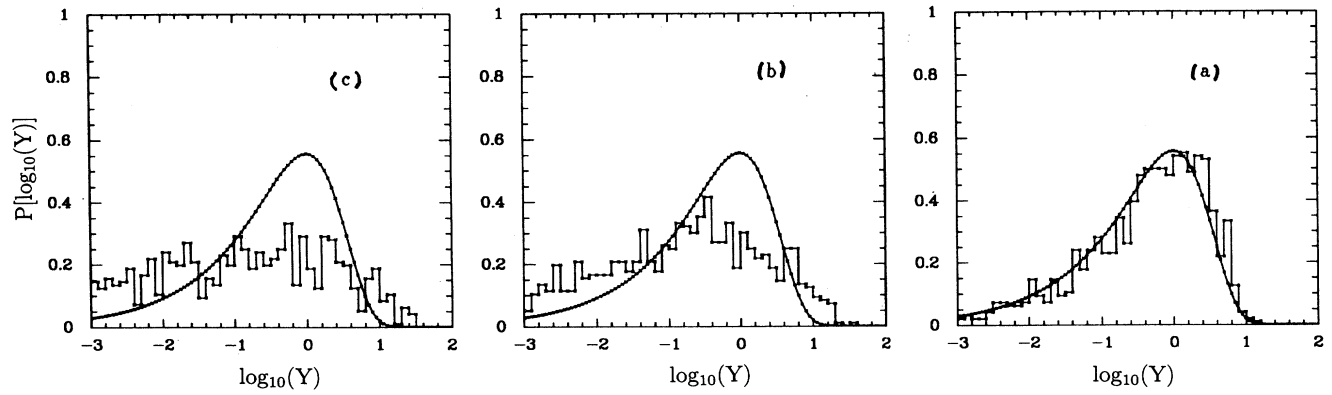


FIG. 3. Same as Fig. 2 but $\lambda=0.25$.

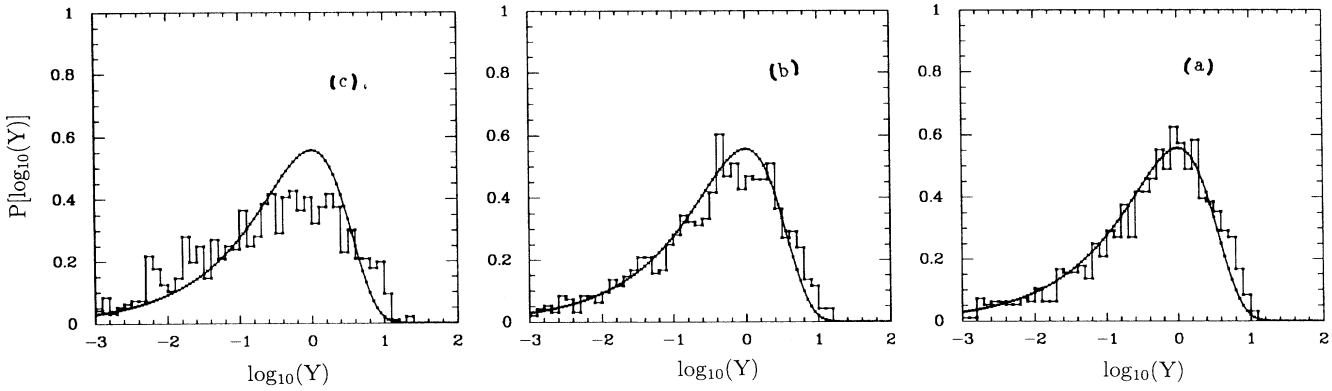


FIG. 4. Same as Fig. 2 but $\lambda=0.48$.

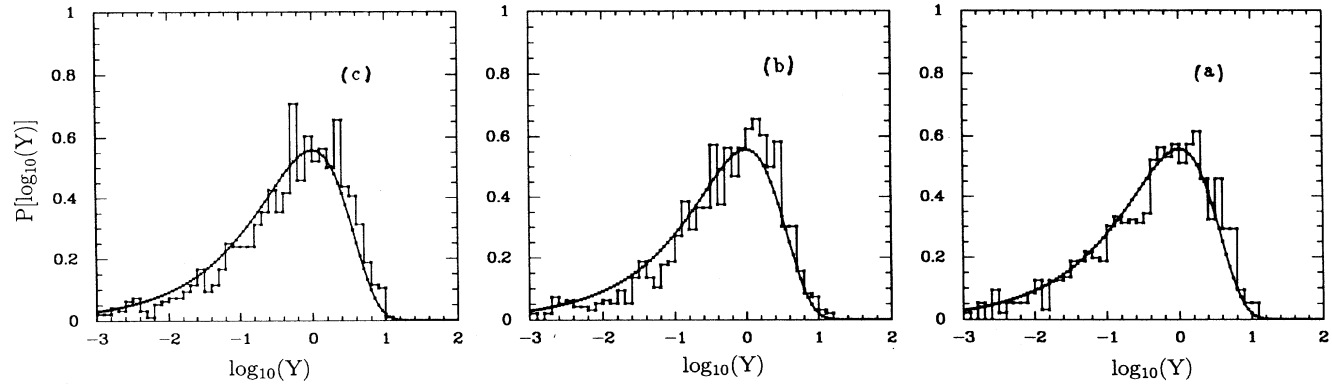


FIG. 5. Same as Fig. 2 but $\lambda=0.78$.

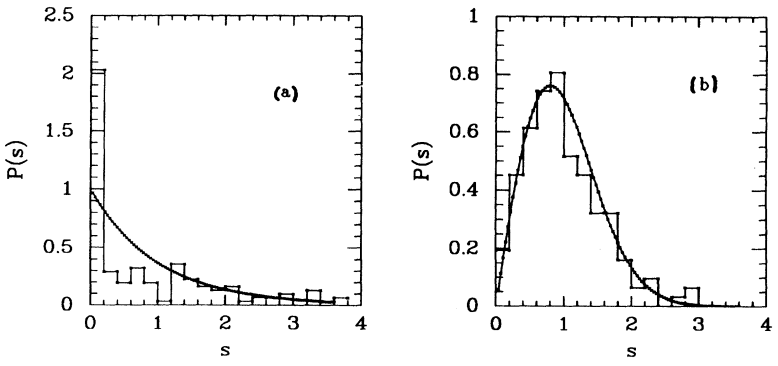


FIG. 6. Spectral statistics for two groups of chosen effective Hamiltonians. (a) is for those whose eigenvector statistics deviate far from the Porter-Thomas distribution. (b) is for those whose eigenvector statistics agree with the Porter-Thomas distribution. The solid lines denote Poission distribution in (a) and Wigner distribution in (b).

Fig. 2, the statistical fluctuations of eigenstates of the effective Hamiltonians related to those three energy regions are all far away from the Porter-Thomas distribution. For the case $\lambda=0.24$ in Fig. 3, the statistics for the energy region with mean energy 20.0 come to agree well with the $\chi^2_{\nu=1}$ distribution, but things about the other two effective Hamiltonians still have little change. In Fig. 4, $\lambda=0.48$, only one energy region gives eigenstate statistics deviating evidently from the $\chi^2_{\nu=1}$ distribution. At last, in Fig. 5, $\lambda=0.78$, the eigenstates statistics of the three effective Hamiltonians all show the $\chi^2_{\nu=1}$ distribution. These results conform with the transition of the spectral statistics from regularity to chaos shown in Fig. 1.

On the other hand, it is difficult to carry out the statistical fluctuations of the eigenvalues of a certain effective Hamiltonian because the dimension is only 31. However, this kind of trouble can be solved by doing the statistical analyses for data from different effective Hamiltonians. Of course, the unfolding process is necessary here. In this way we obtain two types of spectral statistics for two groups of effective Hamiltonians. Figure 6(a) is the result for the effective Hamiltonians corresponding to the histograms in Figs. 2(b), 2(c), 3(b), 3(c), and 4(c), all of which give the eigenvector statistics far away from the Porter-Thomas distribution. As expected, the special statistics obey the Poisson distribution. Analogously, the Wigner distribution in Fig. 6(b) is the result of those effective Hamiltonians whose eigenvector statistics obey the $\chi^2_{\nu=1}$ law. The results of Figs. 6(a) and 6(b) assure us that there are really two types of effective Hamiltonians giving different types of spectral statistics, respectively.

Now we draw the following conclusions.

(i) The effective Hamiltonians related to different energy regions may have distinct statistical behaviors. Effective Hamiltonians having distinct statistical properties may coexist in the same system.

(ii) The effective Hamiltonians giving the $\chi^2_{\nu=1}$ distribution of eigenvector statistics have spectral distributions of the GOE type, while the effective Hamiltonians giving $\chi^2_{\nu\simeq 0}$ distribution of eigenstate statistics have spectral distribution of the Poissonian type.

(iii) Since the randomness property shown by the eigenvector statistics of the $\chi^2_{\nu=1}$ distribution is practically basis independent, the corresponding effective Hamiltonians do fulfill the two requirements of GOE.

(iv) Comparing the results with those in Sec. II, we find that the transition of the spectrum from regularity to irregularity is consistent with the broadening of the energy region over which the statistical properties of the effective Hamiltonians are all random. The intermediate case of the spectral statistics corresponds to the coexistence of effective Hamiltonians with different types of statistical behaviors.

## IV. INVESTIGATIONS OF THE CLASSICAL COUNTERPARTS

The main aim of this section is to provide comparisons of the behaviors in different energy regions between the corresponding classical and quantum cases.

To get the classical counterparts of the quantum system $H(\lambda)$ given by (2)–(6), we first write the Hamiltonian in the boson representation[16],

$$H^0=\epsilon_1 b_1^\dagger b_1+\epsilon_2 b_2^\dagger b_2-\kappa_2\Omega\left[b_2^\dagger\left[1-\frac{1}{\Omega}\sum_i b_i^\dagger b_i\right]^{1/2} b_2^\dagger\left[1-\frac{1}{\Omega}\sum_i b_i^\dagger b_i\right]^{1/2}+\text{H.c.}\right], \tag{26}$$

$$\begin{aligned} V=H-H^0=&-\kappa_1\Omega\left[b_1^\dagger\left[1-\frac{1}{\Omega}\sum_i b_i^\dagger b_i\right]^{1/2} b_1^\dagger\left[1-\frac{1}{\Omega}\sum_i b_i^\dagger b_i\right]^{1/2}+\text{H.c.}\right]\\ &+\mu_1\sqrt{\Omega}\left[b_2^\dagger b_1^\dagger b_2^\dagger\left[1-\frac{1}{\Omega}\sum_i b_i^\dagger b_i\right]^{1/2}+\text{H.c.}\right]+\mu_2\sqrt{\Omega}\left[b_1^\dagger b_2^\dagger b_1^\dagger\left[1-\frac{1}{\Omega}\sum_i b_i^\dagger b_i\right]^{1/2}+\text{H.c.}\right]. \end{aligned} \tag{27}$$

where

$$[b_i,b_j^\dagger]=\delta_{ij},[b_i,b_j]=[b_i^\dagger,b_j^\dagger]=0\ . \tag{28}$$

After transforming the boson creation and annihilation operators $b_i^\dagger,b_j$ to $q_i,p_j$ with

$$b_i^\dagger=\sqrt{\Omega/2}(q_i-ip_i),\quad b_i=\sqrt{\Omega/2}(q_i+ip_i),\quad i,j=1,2 \tag{29}$$

we have

$$[q_i,p_j]=\frac{i}{\Omega}\delta_{ij}\ , \tag{30}$$

so $1/\Omega$ gives us a measure of the quantal effect. If we treat operators $q_i,p_j$ as commutable numbers, i.e., let the particle number $\Omega$ become infinitely large while keeping the following

$$\begin{aligned}&\epsilon_1'=\epsilon_1\Omega,\quad \epsilon_2'=\epsilon_2\Omega,\quad \kappa_1'=\kappa_1\Omega^2\ ,\\ &\kappa_2'=\kappa_2\Omega^2,\quad \mu_1'=\mu_1\Omega^2,\quad \mu_2'=\mu_2\Omega^2\ ,\end{aligned} \tag{31}$$

as constants, the classical counterparts are obtained:

$$H_c(\lambda)=H_c^0+\lambda V_c\ , \tag{32}$$

$$H_c^0=\frac{\epsilon_1'}{2}(p_1^2+q_1^2)+\frac{\epsilon_2'}{2}(p_2^2+q_2^2)-\kappa_2'(p_2^2-q_2^2)\left[1-\frac{p_1^2+q_1^2+p_2^2+q_2^2}{2}\right], \tag{33}$$

$$\begin{aligned}V_c=&-\kappa_1'(p_1^2-q_1^2)\left[1-\frac{p_1^2+q_1^2+p_2^2+q_2^2}{2}\right]+\frac{\mu_1'}{\sqrt{2}}[(p_2^2-q_2^2)p_1+2p_2q_2q_1]\left[1-\frac{p_1^2+q_1^2+p_2^2+q_2^2}{2}\right]^{1/2}\\ &+\frac{\mu_2'}{\sqrt{2}}[(p_1^2-q_1^2)p_2+2p_1q_1q_2]\left[1-\frac{p_1^2+q_1^2+p_2^2+q_2^2}{2}\right]^{1/2}\ .\end{aligned} \tag{34}$$

In order to show the existence or nonexistence of the Kolmogorov-Arnold-Moser (KAM) tori clearly, we use the Poincaré map to investigate the dynamical properties. As illustrated in Figs. 7–10, numerical results in three different energy surfaces with four values of the parameter $\lambda$ are presented. The energy surfaces are chosen to have the same energies as mean energies of the three typical effective Hamiltonians in Sec. III. For the case $\lambda=0.08$ in Fig. 7, almost all the KAM tori are kept. As the perturbation increases to $\lambda=0.24$ in Fig. 8, we see that most of the KAM tori on the energy surface 20.0 are destroyed while those in the other two energy surfaces are only distorted. When $\lambda=0.48$ in Fig. 9, more tori disappear showing the growth of nonintegrability. For the case $\lambda=0.78$ in Fig. 10, with some other detailed numerical results, we find the system is fully chaotic.

Striking, we find good quantum-classical correspondence when comparing the Poincaré maps in Figs. 7–10 with the $\chi_\nu^2$ analyses of eigenvectors of the effective Hamiltonians in Figs. 2–5. The $\chi_{\nu=1}^2$ distribution for eigen-

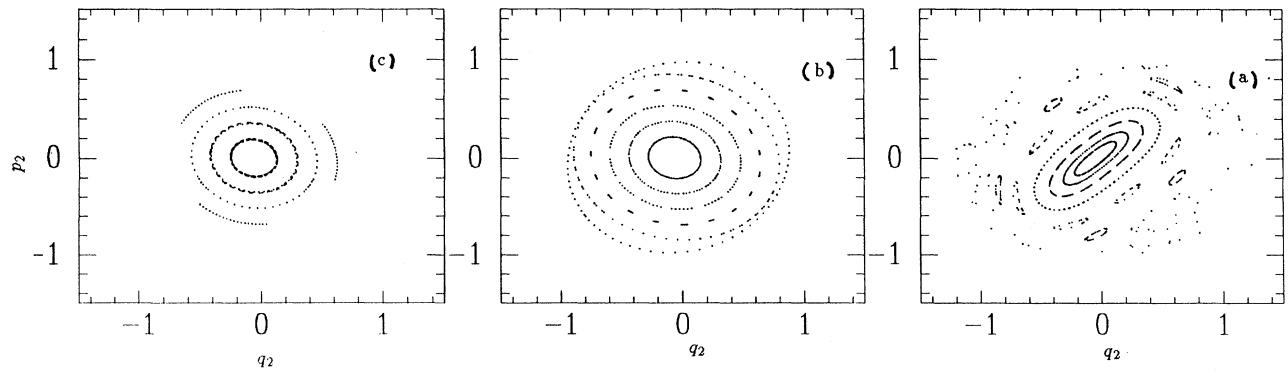


FIG. 7. The Poincaré sections of trajectories for the classical limit of the three-level Lipkin model in the $q_2-p_2$ plane with $p_1>0$ for the case $\lambda=0.08$. Graphs denoted by (a), (b), and (c) are on the energy surfaces with the energies equal to 20.0, 55.0, 75.0, respectively.

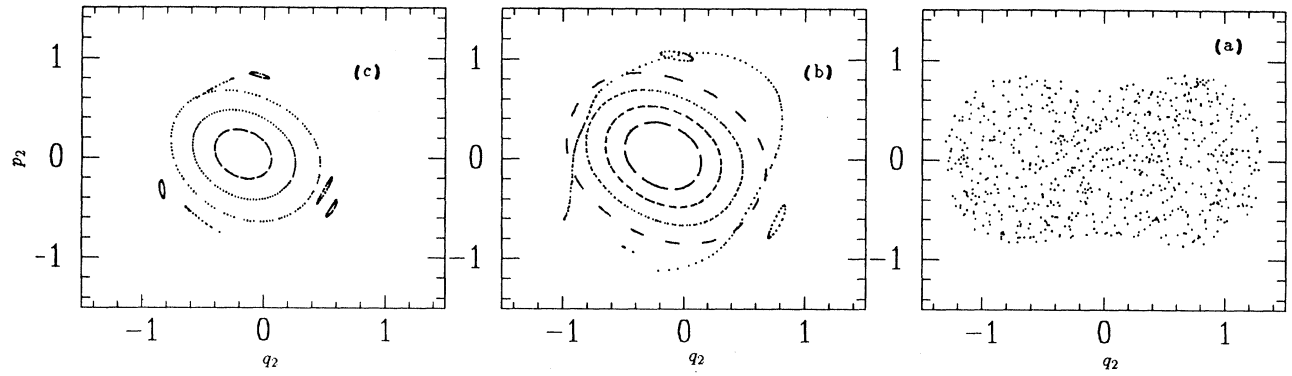


FIG. 8. Same as Fig. 7 but $\lambda=0.24$.

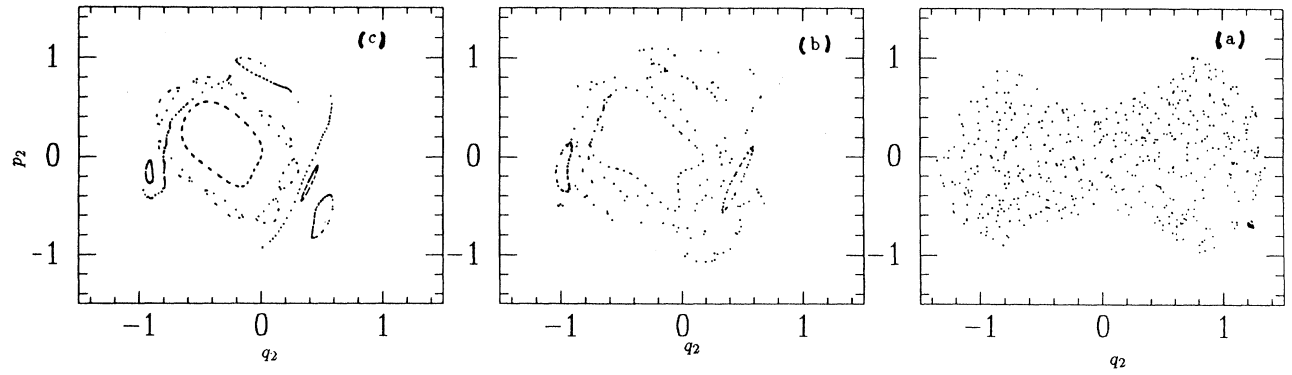


FIG. 9. Same as Fig. 7 but $\lambda=0.48$.

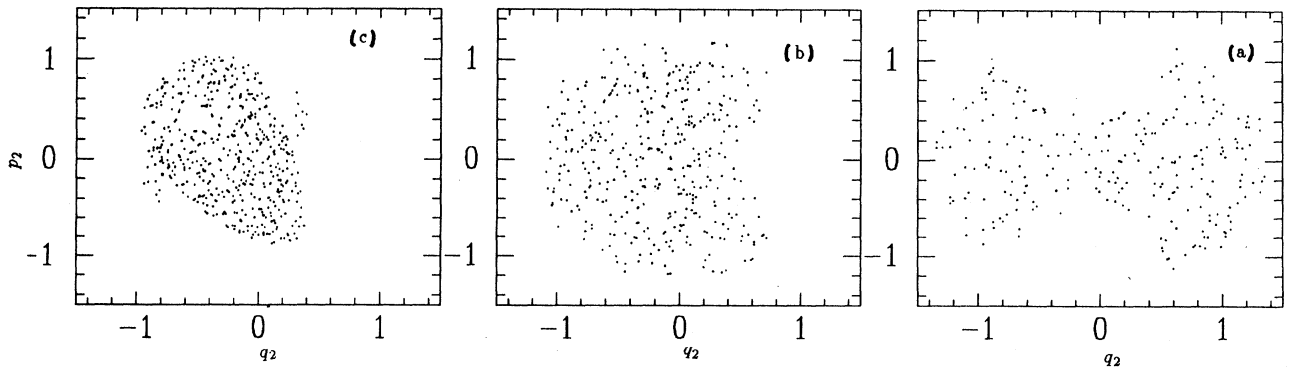


FIG. 10 Same as Fig. 7 but $\lambda=0.78$.

vectors of the effective Hamiltonians are just the local quantum signatures of classical nonintegrability on corresponding energy surfaces, and the evident deviations from the Porter-Thomas distribution imply that almost all KAM tori of the classical counterparts in the relevant energy surfaces remain undestroyed.

The results of this section not only confirm the appropriateness of using effective Hamiltonian matrices for different energy regions to study the transition from regularity to chaos, but also suggest that the broadening of the energy region over which the statistical properties of the effective Hamiltonians are all random is closely related to the development of global nonintegrability as in classical mechanics. We shall discuss this problem in details in the next section.

## V. WHAT IS THE DYNAMICAL BASIS OF GOE?

We shall show in this section that the statistical properties of effective Hamiltonian matrices just come from the dynamical properties of global nonintegrability. We first give an overview about discussions on complete integrability and nonintegrability from our recent articles [15,17].

A system is said to be completely integrable if there exists a complete set of commuting integrals of motion corresponding to a certain subgroup chain of the dynamical group. In such cases the eigenstates $|\phi_i(\lambda)\rangle$ of $H(\lambda)$ can be connected to the initial conditions $|\phi_i^0\rangle$ with a quantum canonical transformation [17]. The eigenstates $|\phi_i(\lambda)\rangle$ retains the main characteristics of $|\phi_i^0\rangle$ and can be designated with the same quantum numbers as for $|\phi_i^0\rangle$; thus $H(\lambda)$ has the same dynamic symmetry as $H^0$.

If there exists perturbation violating the dynamic symmetry, the quantum canonical transformation breaks first at the critical point $\lambda_1$ for a pair of states mixing strongly with each other. The once broken quantum canonical transformation breaks further at subsequent critical points $\lambda_2, \lambda_3, \ldots$ for other pairs of states. If these pairs of states overlap with each other and extend to a global region, such states mixing strongly with each other can only be connected to corresponding initial states with a transformation in a very complicated form involving a very large number of parameters. As a result they are very complicated in nature.

We should note that the above statement refers to an integrable Hamiltonian $H^0$ corresponding to a definite subgroup chain. A system which is not integrable in reference to a certain subgroup chain may still be integrable in reference to another subgroup chain. But a system is nonintegrable in a global region only if the system is not integrable in this region with respect to all subgroup chains.

The information entropy

$$S_i = -\sum_k |\langle \phi_j^0 | \phi_i(\lambda) \rangle|^2 \ln |\langle \phi_j^0 | \phi_i(\lambda) \rangle|^2 \tag{35}$$

for eigenvectors is a good measure of their respective distributedness. The distributedness $M$ of eigenvectors in a certain energy region can be estimated with the following expression [18]:

$$M = 2 \exp \left[ \bar{S} + \Psi \left[ \frac{\nu}{2} + 1 \right] \right] , \tag{36}$$

where $\bar{S}$ denotes the mean value of $S_i$ in the energy region and $\Psi((\nu/2)+1)$ is the diagamma function. $\nu = 1$ for time-reversal invariant systems. The effective Hamiltonian for a $\Delta N$-dimensional energy region obtained with the decoupling transformation has already carried information from states lying outside the region but strongly coupled to those inside the region. If $\Delta N \ll M$, the effective Hamiltonian of the region should be in a very complicated form involving a large number of parameters much exceeding the number of independent elements of the effective Hamiltonian matrix. The elements of the effective Hamiltonian matrix will then appear as uncorrelated random quantities. On the other hand, $\Delta N$ cannot be chosen arbitrarily small. In order to deal with properties of eigenstates in the region statistically, we must have $1 \ll \Delta N$. Hence there exists a condition for the randomness of effective Hamiltonian matrices

$$1 \ll \Delta N \ll M . \tag{37}$$

The calculated results of distributedness for different model parameters and different energy regions corresponding to Figs. 2–5 are given in Table I. Noticing $\Delta N = 31$ for the present case, we see clearly that for energy regions corresponding to Figs. 3(a), 4(a), 4(b), 5(a), 5(b), 5(c) with the statistics of eigenvectors of the corresponding effective Hamiltonians obeying the Porter-Thomas distribution, the condition (37) is indeed satisfied, while for regions corresponding to Figs. 2(a), 2(b), 2(c), 3(b), 3(c), 4(c) having quite different features, $M \lesssim \Delta N$, the condition (37) is not satisfied.

Moreover, the introduction of the effective Hamiltonian is also essential for removing the smoothly varying mean properties of subregions inside the same nonintegrable region. If $M$ is sufficiently large comparable with $N$, it is unsuitable to consider just the effective Hamiltonian in this $M$-dimensional subspace. The eigensolutions in this region have lost all possible regularities except their mean properties which still vary smoothly in this region. Of course the eigenenergies should be unfolded. Besides, the eigenstates may have their components distributed almost randomly over the whole space but more or less

TABLE I: The averaged distributedness $M$ of eigenvectors in three energy regions for four values of the parameter $\lambda$, the same as in Figs. 2–5.

| Parameters | $\bar{E}=75.0$ | $\bar{E}=55.0$ | $\bar{E}=20.0$ |
|---|---|---|---|
| $\lambda=0.08$ | 6.7 | 11.0 | 44.2 |
| $\lambda=0.24$ | 29.8 | 77.6 | 192.4 |
| $\lambda=0.48$ | 99.2 | 199.6 | 299.5 |
| $\lambda=0.78$ | 204.4 | 311.6 | 375.5 |

concentrated at their original locations. Only after these local mean properties have been removed with the appropriate unfolding process, can the eigenenergies and eigenvectors be treated as random quantities.

As eigenenergies and eigenvectors are obtained at the same time, the unfolding process for eigenvectors should conform with that for eigenenergies. This can be attained by considering the effective Hamiltonians in different energy regions. Then the variation of local mean properties of eigenvectors viewed from the $M$-dimensional subspace no longer appears in the analyses of eigenvectors in the $\Delta N$-dimensional regions. Suppose $D_\mu$ is the mean energy spacing of region $\mu$. We define the unfolded effective Hamiltonians as follows:

$$\overline{H}_{\text{eff},\mu}(\lambda)=\frac{1}{D_\mu}[H_{\text{eff},\mu}(\lambda)-E_\mu I] . \tag{38}$$

Now $\overline{H}_{\text{eff},\mu}$ for different regions have only random properties besides the common mean energies and mean energy spacings and can be treated as members of GOE. This provides a precise understanding of the random-matrix theory.

To end this section, we should like to refer to the paper by Meredith, Koonin, and Zirnbauer [13]. In a similar three-level Lipkin model, they found systematic deviations from GOE in the statistics of eigenvector overlaps with original basis states while the eigenvalue statistics are in good agreement with GOE. According to our calculations, this dilemma can be resolved by using the effective Hamiltonians. Then, both the eigenvalue statistics and the eigenvector statistics agree with GOE.

## VI. CONCLUSIONS

Now we draw conclusions based on the above-mentioned numerical results as follows.

(i) In treating the eigenvectors and eigenenergies statistically, effective Hamiltonians for different energy regions should be introduced such as to distinguish integrable and partly integrable regions from chaotic ones and to remove the smoothly varying mean properties.

(ii) The unfolded effective Hamiltonians $\overline{H}_{\text{eff},\mu}$ for nonintegrable regions having only random properties besides the common mean energy and mean level spacings are taken as members of GOE. With them, spectral statistics and eigenvector statistics are obtained in good correspondence to parallel results of classical counterparts.

(iii) The randomness property of $\overline{H}_{\text{eff},\mu}$ comes basically from dynamical properties of nonintegrability in the region $\mu$ subject to the condition (37).

We should like to note that it requires further studies to show whether our results are indeed universal by using other models or by more elaborate theoretical considerations. We are working in this direction.

## ACKNOWLEDGMENTS

The authors thank Professor J. D. Garrett for helpful discussions. One of the authors (Gong Jiang-bin) also appreciates Professor Huang Jie-hao and Professor Zhou Qin-lin for beneficial help in the process of numerical experiments. This work was supported by the National Basic Research Project "Nonlinear Science," China, Natural Science Foundation of China, and Natural Science Foundation of Jiangsu, China.

[1] *Statistical Theories of Spectra: Fluctuations,* edited by C. E. Porter (Academic, New York, 1965).
[2] M. V. Berry and M. Tabor, Proc. R. Soc. London Ser. A **356**, 375 (1977).
[3] M. C. Gutzwiller, *Chaos in Classical and Quantum Mechanics* (Springer-Verlag, New York, 1990) p. 275.
[4] M. V. Berry and M. Robnik, J. Phys. A **17**, 2413 (1984).
[5] T. A. Brody, Lett. Nuovo Cimento **7**, 482 (1971).
[6] N. Whelan, Y. Alhassid, and A. Levitan, Phys. Rev. Lett. **71**, 2208 (1993).
[7] Wang Wen-ge, Ph.D. thesis, Nanjing University, China, 1992.
[8] R. U. Haq, A. Pandey, and O. Bohigas, Phys. Rev. Lett. **48**, 1086 (1982).
[9] J. D. Garrett, J. R. German, L. Courtney, and J. M. Espins, in *Future Directions with* $4\pi$ *Gamma Detection Systems of the New Generation,* edited by J. Dudek and B. Haas (AIP, New York, 1991) p. 345.
[10] B. A. Brown and G. Bertsch, Phys. Lett. **148B**, 5 (1984).
[11] M. Zirnbauer, J. Verbaarschot, and H. Weidenmiiller, Nucl. Phys. A **411**, 621 (1983).
[12] J. B. French, V. K. Kota, A. Pander, and S. Tomsovie, Ann. Phys. (N.Y.) **181**, 198 (1988).
[13] D. C. Meredith, S. E. Koonin, and M. R. Zirnbauer, Phys. Rev. A **37**, 3499 (1988).
[14] H. J. Lipkin, N. Meshkov, and A. J. Glick, Nucl. Phys. **62**, 188 (1965).
[15] Xu Gong-ou, Wang Wen-ge, and Yang Ya-tian, Phys. Rev. A **45**, 540 (1992).
[16] Xu Gong-ou, Wang Shun-jing, and Yang Ya-tian, Phys. Rev. C **36**, 2095 (1987).
[17] Xu Gong-ou *et al.* (unpublished).
[18] G. Casati, I. Guarneri, F. Izrailev, and R. Scharf, Phys. Rev. Lett. **64**, 5 (1990).